Comparison of Three Popular PLL Schemes under Balanced and Unbalanced Grid Voltage Conditions

Iwan Setiawan[1], Mochammad Facta[2]
Department of Electrical Engineering
Universitas Diponegoro, Semarang, Indonesia
[1]setiaone.iwan@gmail.com
[2]mochfacta@gmail.com

Ardyono Priyadi[3], Mauridhi Hery Purnomo[4]
Department of Electrical Engineering
Institut Teknologi Sepuluh Nopember Surabaya, Indonesia
[3]priyadi@ee.its.ac.id
[4]hery@ee.its.ac.id

***Abstract*—The aims of this paper is to study and to compare the performance of the three most likely popular PLL strategies that could be found in renewable on-grid power generation control systems: SRF-PLL, DSRF-PLL and DSOGI-PLL. In the on-grid power generation, The PLL has responsibility to acquire grid phase angle and positive-negative sequence components of the grid voltage vector which are required for syncronization process between the grid side converter system with the grid. By performing simulations under Matlab/Simulink environment and analize the results. It is shown that under balanced grid voltage conditions, the performance of the SRF-PLL is more superior compared to two other methods, however for unbalanced conditions, the best output performance is resulted by the DSOGI-PLL.**

Keywords— Phase Locked Loop; DSRF-PLL; DSOGI-PLL; unbalanced voltage conditions; SRF-PLL

I. INTRODUCTION

In recent years, the penetration of distributed green power generation systems have been taking place rapidly. Through a converter power electronic system, that is well-known as a grid side converter - GSC and its associated controller, the electrical power from renewable power generation systems such as tydal, sea wave, wind and solar power are injected to the grid [1-5].

Based on the grid connection requirements, the GSC should be able to operated and connected to the grid even if the grid is experiencing interference which are caused by several conditions, such as: connections and disconnections of relatively large electrical loads, grid voltage unbalance and harmonics. To achieve this purposes, the GSC control system technically should have ability to detect grid disturbances quickly so that the grid voltage information such as the phase angle and the sequence components of the grid voltage vector which are required by the main control system of the GSC remain available accurately and in real time fashion.

The component responsible for providing a variety of the grid voltage information to the GSC control system is well-known as a phase locked loop (PLL) feedback system. Fig.1 shows a simplified block diagram of the PLL in a typical renewable on-grid power generation system. Besides have main role in the GSC, the PLL is also could be found in several devices, such as: active AC/DC converters[6-7], On-Grid inverter system [8], FACT devices and HVDC systems [9-10].

Although there are many PLL topologies which are proposed in literatures[11-13], however in practice only a few which popular due to their relatively simple structure and their performances. The aims of this paper is to investigate of several most popular PLLs: Synchronous reference frame-phase locked loop (SRF-PLL), dicouple double synchronous reference frame-phase locked loop (DDSRF-PLL) and dicouple double second order general integrator-phase locked loop (DSOGI-PLL) in response to the grid voltage magnitude changes, both symetrical and asymetrical changes. The voltage magnitude changes basically is general phenomenon that can be found in rural or remote areas in which renewable power generation systems are installed. By this study, the appropriate PLL topology can be chosen based on the GCS controller requirement

The remainder of this paper is organized as follows. Section 2 describes the short theory of the generalized unbalanced voltage conditions. In Section 3, several popular PLL topologies will be discussed at glance, next, Section 4 shows the simulation results and discuss the transient and steady state performance of the PLLs. Finally, the conclusions of the study are drawn at Section 5.

II. GENERALIZED UNBALANCED GRID VOLTAGE REPRESENTATION

In the complex vector form, The representation of the voltage under balanced conditions is shown in (1).

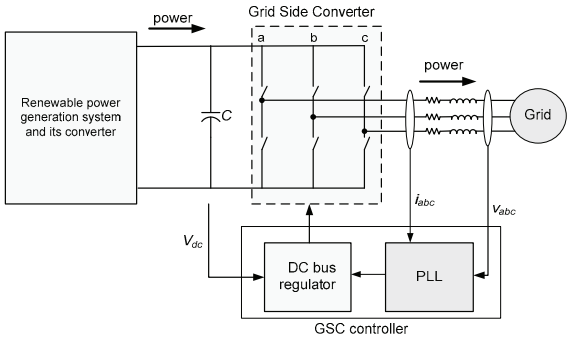

Fig.1. The GSC in a renewable on-grid power generation system

978-1-5090-4139-8/16/$31.00 ©2016 IEEE

$$\bar{v}_s = (v_+)e^{j\omega t} \quad (1)$$

where $\bar{v}_s$ is a voltage vector that represented in the stationary reference frame :

$$\bar{v}_s = v_\alpha + jv_\beta \equiv 2/3\left(v_a(t) + v_b(t)e^{j2\pi/3} + v_c(t)e^{j4\pi/3}\right) \quad (2)$$

whereas v_+ and $e^{j\omega t}$ respectively are a voltage vector in a rotating reference frame: $v_+ = v_{d+} + jv_{q+}$ and a unit vector that is rotated at ω rad/sec in the counterclockwise direction. In matrix-vector relations, the vector component of $\bar{v}_s$ and v_+ respectively could be found from the well-known Clarke and Park transformations below:

$$\begin{bmatrix} v_\alpha \\ v_\beta \end{bmatrix} = \frac{2}{3}\begin{bmatrix} 1 & -1/2 & -1/2 \\ 0 & \sqrt{3}/2 & -\sqrt{3}/2 \end{bmatrix}\begin{bmatrix} v_a \\ v_b \\ v_c \end{bmatrix} \quad (3)$$

$$\begin{bmatrix} v_{d+} \\ v_{q+} \end{bmatrix} = \begin{bmatrix} \cos\theta & \sin\theta \\ -\sin\theta & \cos\theta \end{bmatrix}\begin{bmatrix} v_\alpha \\ v_\beta \end{bmatrix} \quad (4)$$

Where $\theta=\omega t$ is the grid voltage phase angle.

Whereas the grid voltage under unbalanced conditions mathematically are composed from two vectors which rotated in opposite direction at the angular frequency ω rad/sec as shown by (5).

$$\bar{v}_s = (v_+)e^{j\omega t} + (v_-)e^{-j\omega t} \quad (5)$$

Where $v_- = v_{d-} + jv_{q-}$. By multiplied $\bar{v}_s$ at (5) respectively by $e^{-j\omega t}$ and $e^{j\omega t}$, the voltage expressions in the positive and negative synchronous reference frame respectively could be represented as shown in (6) and (7).

$$\bar{v}_s e^{-j\omega t} = (v_+) + (v_-)e^{-j2\omega t} \quad (6)$$

$$\bar{v}_s e^{j\omega t} = (v_-) + (v_+)e^{j2\omega t} \quad (7)$$

From (6) and (7), it is clear that both of the positive and negative sequence components of the grid voltage under unbalance conditions will experience oscillation by angular frequency 2ω rad/sec. In this case, the negative sequence component will appear as 2ω rad/sec in the positive sequence of the voltage vector and vice versa, the positive sequence component will appear as 2ω rad/sec in the negative sequence of the voltage vector. Eq. (8) and (9) respectively show the voltage vector components in the positive and negative synchronous reference frame.

$$\begin{bmatrix} v_{ud+} \\ v_{uq+} \end{bmatrix} = \begin{bmatrix} v_{ud+} \\ 0 \end{bmatrix} + \begin{bmatrix} v_{d-}\cos(-2\omega t) \\ v_{q-}\sin(-2\omega t) \end{bmatrix} \quad (8)$$

$$\begin{bmatrix} v_{ud-} \\ v_{uq-} \end{bmatrix} = \begin{bmatrix} v_{ud-} \\ 0 \end{bmatrix} + \begin{bmatrix} v_{d+}\cos(2\omega t) \\ v_{q+}\sin(2\omega t) \end{bmatrix} \quad (9)$$

III. PLL METHODS

In on-grid converter systems, the information of the voltage vector components both in the positive and negative synchronous reference frame and the phase angle are crucial for syncronization process of the control system operation. The component which has responsibility to acquire those information is a PLL. The PLL basically is a feedback control system which regulate a locally signal phase to match with a input signal phase. In a three phase grid system, the PLL is used to synchronize the operation of the grid-connected device with the grid. Three types of the PLL will be discussed in this section: SRF-PLL, DSRF-PLL and DSOGI-PLL.

A. SRF-PLL

Compared to other PLL algorithms, the SRF-PLL is likely the most popular PLL type in practice. Fig. 2 shows a diagram block of the SRF-PLL. From Fig. 2 it is shown that the SRF-PLL is basically composed from two main computation blocks: (1) Clark and Park transformation blocks and (2) a proportional integral (PI) feedback control system. In the SRF-PLL scheme, the Clark and Park transformation blocks change a representation of the three phase variable: v_a,v_b, and v_c to ortogonal variables: v_d and v_q in a positive rotating synchronous reference frame. Whereas the standard PI feedback controller with a feedfoward bias-ω_{ff} (nominal grid frequency) is used to nulling the quadrature component of the grid voltage (v_q), so that in every moment will be obtained synchronization between a *d-q* reference frame with the rotating *α-β* voltage vector as shown in Fig.3.

by using proper PI parameters, then the grid voltage variables, such as the phase angle, frequency, and grid voltage magnitude could be obtained. However due to the SRF- PLL just handle the positive sequence component of the grid voltage, this PLL will be suffer from unbalanced voltage conditions. In this case, the operation of SRF-PLL under unbalanced grid voltage conditions will result fluctuations both in the voltage and in the frequency.

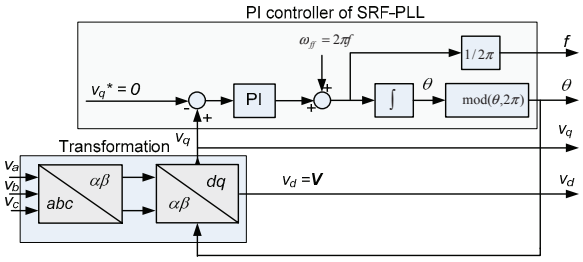

Fig.2. SRF-PLL block diagram

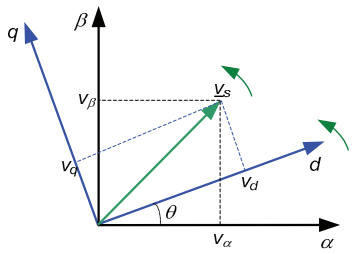

Fig.3. grid voltage synchronization

B. DSRF-PLL

Differ from the SRF-PLL that just handle the positive sequence of the grid voltage, in the DSRF-PLL scheme, both of the grid voltage sequences are handled simultaneously so that the DSRF-PLL could estimate the positive and negative sequences of the grid voltage vector under generilized unbalanced grid voltage conditions. Fig. 4 shows building block of the DSRF-PLL. As shown in Fig.4, the DSRF-PLL works in the *d-q* synchronous rotating frame.

In the DSRF-PLL scheme, the voltage vector in the stationary reference frame: v_α and v_β are projected respectively on to a positive and negative rotating reference frame to obtain the positive and negative sequence component of the voltage vector. The main role of the cross decoupling blocks that shown in detail at Fig. 5 and Fig. 6 is to eliminate coupling between the positive and negative sequence of the voltage in each rotating reference frame, whereas the low pass filter (LPF) in this case is to smooth the output signals mainly in the transient state. For the detail explanation, the reader could be refer to [14[[15].

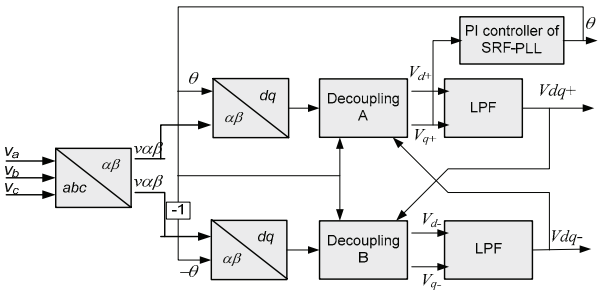

Fig.4. DSRF-PLL block diagram

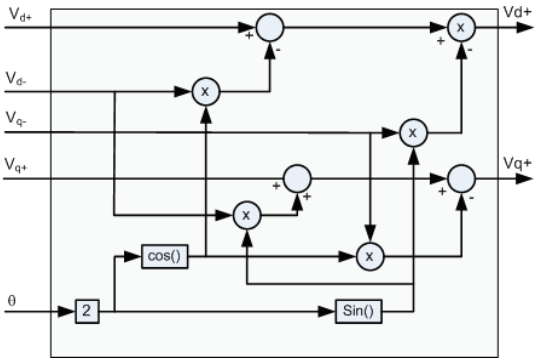

Fig.5. Decoupling A block diagram in DSRF-PLL

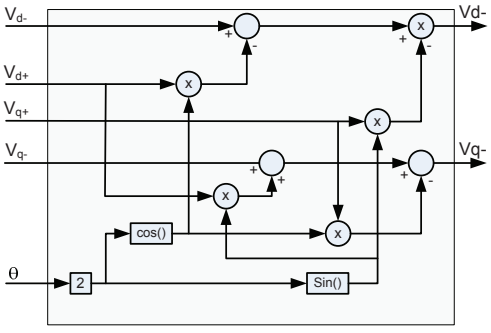

Fig.6. Decoupling B block diagram in DSRF-PLL

C. DSOGI-PLL

Fig. 7 shows the diagram block of the DSOGI-PLL. As shown in the Fig. 7, there are four main functional blocks in this type of the PLL: (1) Clark transformation, (2) Second Order Generalized Integrator – Quadrature Signal Generator (SOGI-QSG), (3) Positive-Negative Signal Calculator (PNSC) and (4) Synchronous Reference Frame-Phase Locked Loop (SRF-PLL) both for positive and negative sequence component of the grid voltage.

In the DSOGI-PLL, two quadrature signal generators (QSG) based on the second order generalized integrator (SOGI) is employed to generate orthogonal signals both for v_α and v_β. Fig. 8 show the detail algorithm for SOGI-QSG. In this algorithm, ω_{ff} is the nominal value of the grid frequency that acting as a feedfoward control variable. However, by using the constant ωff , the performance of the SOGI-QSG will be degraded if the grid frequency is deviated from the nominal.

As shown at Fig.9, the pair of quadrature signals is further enter to the positive-negative sequence calculator (PNSC) block. In this case, the PNSC is responsible to extract the positive and negative sequence component of the grid voltage in the stationary reference frame. To obtain the positive and negative sequence component of the grid voltage in the rotating reference frame, the signals are then fed to the SRF-PLL.

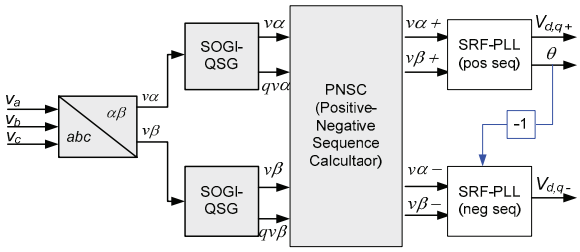

Fig.7. DSOGI-PLL block diagram

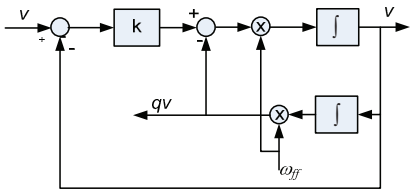

Fig.8. SOGI-QSG block diagram

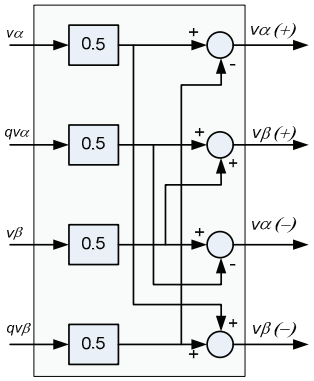

Fig.9. PNSC block diagram

IV. SIMULATION AND DISCUSSIONS

In this section, the three different strategies of the PLLs are evaluated and compared by Simulation models that run under Matlab-Simulink environment. Table 1 shows the parameters of the grid and PLL which is used in this simulation. The performance of the each PLL is measured based on the PLL output transient response due to balanced voltage change as well as unbalanced voltage change.

A. Balance Voltage Changes

Fig.10 shows the grid voltage profile with symetrical voltage change which is used in the simulation. As shown in the plots, at the initial time of the simulation, the magnitude of the grid voltage is 310 Volt, then at about t=0.58s , all of the phase voltages fall down to 220 Volt. For this voltage changes, the PLL output responses are shown at Fig.11 until Fig.13.

Table 1. Parameters of the grid and PLL

No	Parameter	Value
1	Nominal grid frequency-Hz	50
2	Nominal voltage magnitude-line to netral-Volt	310
3	K_p (in SRF-PLL)	10
4	T_i (in SRF-PLL)	20
5	Low pass Filter-cut off frequency-Hz (in DSRF-PLL)	50
6	k (in DSOGI)	1.4

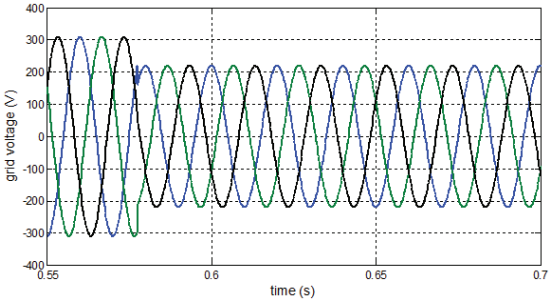

Fig. 10. Symmetrical grid voltage change

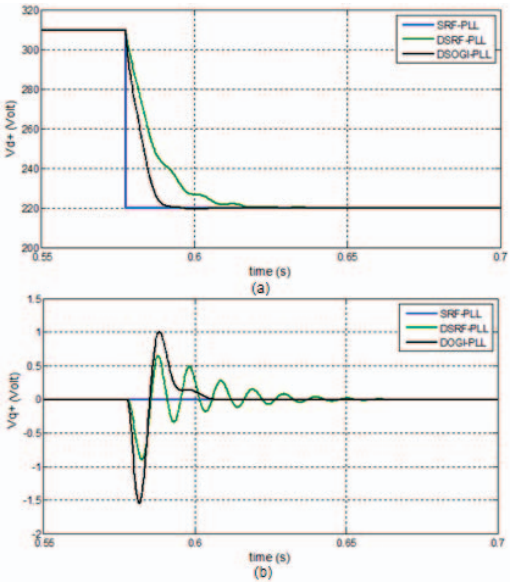

Fig. 11. Transient response of the positive sequence components of the voltage: (a) direct-axis (b) quadrature axis

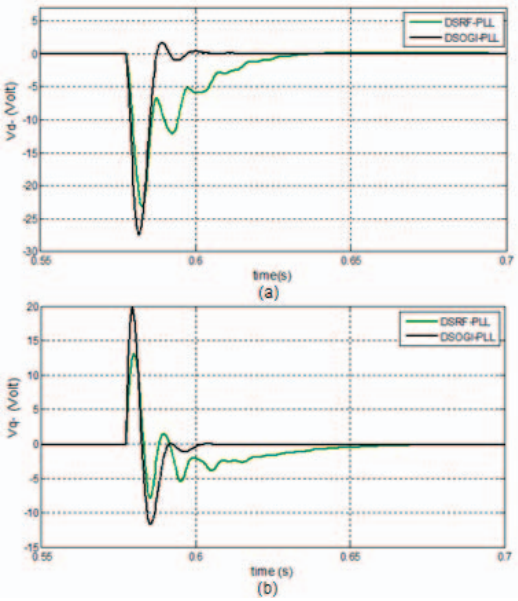

Fig. 12. Transient response of the negative sequence components of the voltage: (a) direct-axis (b) quadrature axis

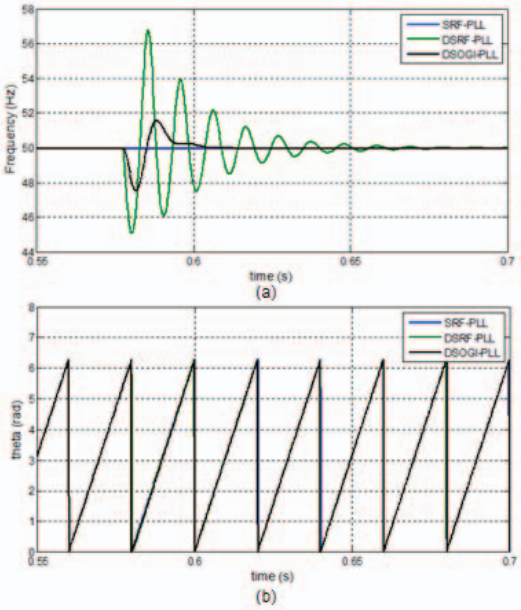

Fig. 13. Transient response of the frequency (a) and phase angle (b)

Fig. 11(a) and Fig. 11(b) respectively show the transient response of the positive sequence components of the grid voltage resulted from the three different PLL strategies due to the voltage changes depicted at Fig. 10. From those plots, it is clear that the transient response of the direct and quadrature axis voltage resulted from three PLL schemes are relatively different: Compared to DSRF-PLL and DSOGI-PLL, the transient performance of the SRF-PLL is look more superior. In this case, the output response of the SRF-PLL have very fast transient response to the change of the grid voltage. From the three plots, the transient response of the DSRF-PLL is more sluggish and more oscillate.

Fig. 12(a) and Fig. 12(b) respectively show the transient response of the negative sequence components of the grid voltage resulted from the DSRF-PLL and DSOGI-PLL

strategies due to the voltage changes depicted at Fig.10 (by refer to its topology, there is not negative sequence component resulted by the SRF-PLL) . From the plots, it is clear that although the overshoot in response to step change for the DSOGI is higher than the DSRF-PLL, however the transient performance of the DSOGI-PLL output in response to voltage changes in general is faster and more stable compared to the DSRF-PLL.

Fig. 13(a) and Fig. 13(b) respectively show the frequency outputs and phase angles detected by the three PLL in response to voltage change-Fig 10. As shown in Fig. 13(a), the frequency output of the SRF-PLL in response to symmetrical voltage change is almost not influenced. Compared to other methods, the frequency output of the DSRF is very sensitive to the voltage change.

B. Unbalance Voltage Change

Fig. 14 shows the grid voltage profile for the simulation purposes. As shown in the plot, at the initial time of simulation, the magnitude for all the phase voltage are 310 volt. Then at simulation time t=0.56s , the phase voltage v_a fall down to 220 volt, whereas the phase voltage v_b and v_c are remain the same. The PLL output responses for this voltage change are shown respectively at Fig.15 to Fig.18.

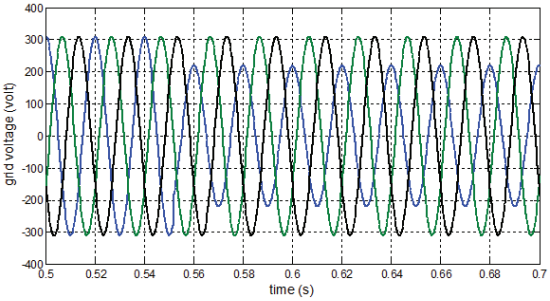

Fig. 14. Unsymmetrical grid voltage change

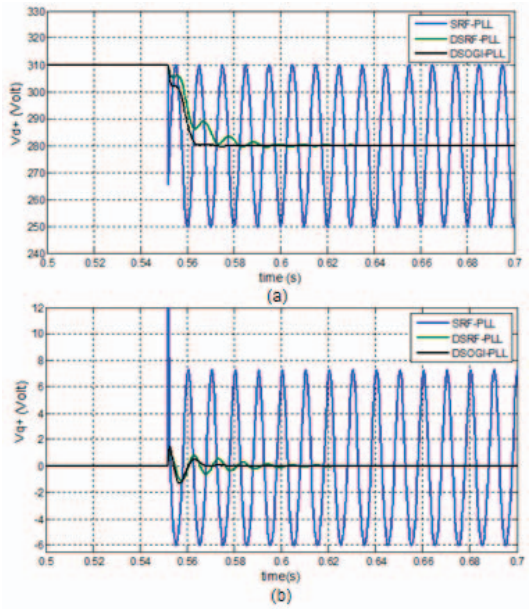

Fig. 15. Transient response of the positive sequence components of the voltage: (a) direct-axis (b) quadrature axis

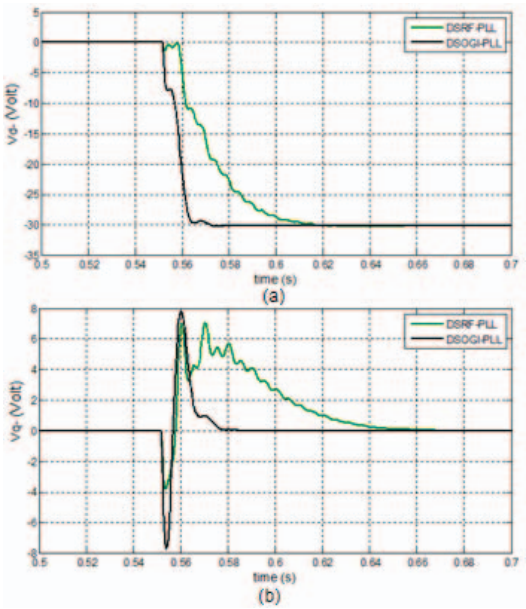

Fig. 16. Transient response of the negative sequence components of the voltage: (a) direct-axis (b) quadrature axis

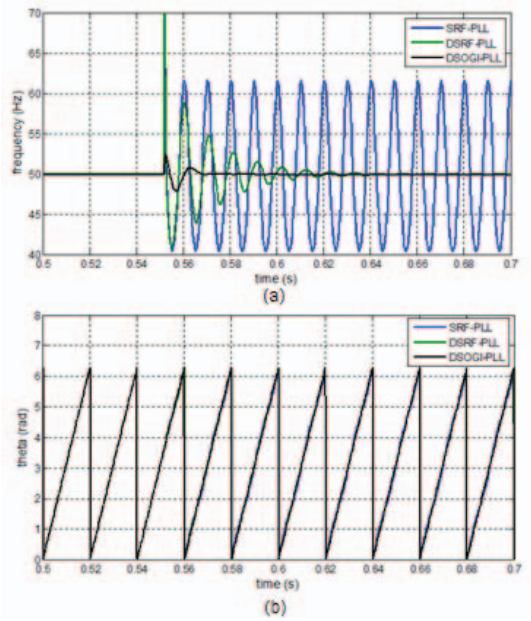

Fig. 17. Transient response of the frequency (a) and phase angle (b)

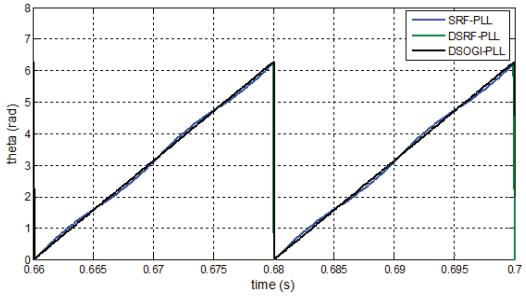

Fig. 18. Transient response of the frequency (a) and phase angle (b)

Fig. 15(a) and Fig. 15(b) respectively show the responses of the positive-sequence components of the grid voltage

resulted from estimation of the SRF-PLL, DSRF-PLL and DSOGI-PLL strategies for grid voltage profile depicted at Fig. 14. It is clear from those plots that at the steady state, the direct and quadrature-axis voltage resulted in the unsymetrical voltage change for the SRF-PLL schemes are experiencing oscillation at the angular frequency 100π rad/sec. This magnitude oscillations basically came from the result of oppositely rotating vectors as represented at (8).

Whereas for this unbalanced voltage change, the steady state responses of the DSRF-PLL and DSOGI-PLL as shown at the Fig. 15 are almost constant. This indicated that both PLL have capability to detect the true value of the positive sequence components of the grid voltage under unbalanced conditions. From the plots of Fig.15, it is also shown that at the transient state, the performance of the DSOGI-PLL is look more supperior than the DSRF-PLL. In this case, the output response of the DSOGI-PLL need less time to settle at the new value.

Fig. 16(a) and Fig. 16(b) respectively show the negative-sequence component output of the DSRF-PLL and DSOGI-PLL strategies in response to the unbalanced voltage changes depicted at Fig.14. As the positive-sequence component response in Fig.5, from the plots it is clear that the DSOGI-PLL output have the fast transient time to settle in the new value compared to DSRF-PLL.

Fig. 17(a) show the frequency outputs estimated by the three PLL in response to unsymmetrical voltage change-Fig 14. As shown at the plots, due to the SRF-PLL could only handle voltage changes under balanced conditions, then the frequency output of the SRF-PLL under unbalanced condition in the steady state would suffer from fluctuation, whereas the frequency estimation of the DSRF-PLL and DSOGI-PLL in this case are almost not influenced by the unsymmetrical voltage change.

Fig.17(b) shows the phase angle estimated the three PLL strategies in response to the voltage chnge under unbalanced conditions. In this case , the zoomed version of the responses is shown in Fig. 18. From the plots it is shown that the phase angle output of the DSRF-PLL and the DSOGI-PLL in the steaady state are almost unaffected by the unbalance voltage condition, however as shown at the plots, the SRF-PLL fails to remain in steady state and suffers from oscillations.

V. CONCLUSION

In this paper, we have shown the capability of the SRF-PLL, DSRF-PLL and DSOGI-PLL to extract grid voltage information, such as phase angle, positive-negative sequence component of grid voltage vector and frequency under generalized unbalanced voltage conditions. From the simulation result, it is shown that under balanced voltage condition, the grid voltage information are best estimated by the SRF-PLL, however under unbalanced conditions the SRF-PLL is failed to estimate the true information of the grid voltage parameter. Under unbalanced conditions, the phase angle, sequence component of the voltage and frequency could be estimated relative accurate by using the DSOGI-PLL.

ACKNOWLEDGMENT

This research was supported by RPP-Universitas Diponegoro [1051-127/UN7.5.1/PG/2016]

REFERENCES

[1] Westwood, Adam. "Ocean power: Wave and tidal energy review." Refocus 5.5 (2004): 50-55.

[2] Lomerson Sr, Robert B., and Robert B. Lomerson Jr. "Tidal power generation." U.S. Patent No. 7,199,483. 3 Apr. 2007.

[3] Kimoulakis, Nikolaos M., Antonios G. Kladas, and John A. Tegopoulos. "Power generation optimization from sea waves by using a permanent magnet linear generator drive." Magnetics, IEEE Transactions on 44.6 (2008): 1530-1533.

[4] Setiawan, Iwan, Ardyono Priyadi, and Mauridhi Hery Purnomo. "Control Strategy Based on Associative Memory Networks for a Grid-Side Converter in On-Grid Renewable Generation Systems Under Generalized Unbalanced Grid Voltage Conditions." *International Review of Electrical Engineering (IREE)* 11.2 (2016): 171-182.

[5] Esram, Trishan, and Patrick L. Chapman. "Comparison of photovoltaic array maximum power point tracking techniques." IEEE Transactions on Energy Conversion EC 22.2 (2007): 439.

[6] Purnomo, M. Hery, and M. Ashari. "High Performance of Nonlinear Active Rectifier Voltage and Power Factor Control Using Feedback Linearization." International Review of Electrical Engineering (IREE) 8.2 (2013): 568-575.

[7] J. W. Kolar and T. Friedli, "The essence of three-phase PFC rectifier systems," in Proc. IEEE Int. Telecom. Energy Conf., 2011, pp. 1–27.

[8] Handoko, S., Sasongko P. Hadi, and Firmansyah,E.. "Parameter Optimization of Proportional Integral Controller in Three-Phase Four-Wire Grid Connected Inverter using Ant Colony Optimization" *Journal of Theoretical & Applied Information Technology* 73.3 (2015).

[9] Messina, A. R., M. A. Perez, and E. Hernandez. "Co-ordinated application of FACTS devices to enhance steady-state voltage stability." International journal of electrical power & energy systems 25.4 (2003): 259-267.

[10] Ding, Guanjun, et al. "New technologies of voltage source converter (VSC) for HVDC transmission system based on VSC." Power and Energy Society General Meeting-Conversion and Delivery of Electrical Energy in the 21st Century, 2008 IEEE. IEEE, 2008.

[11] Blaabjerg, Frede, et al. "Overview of control and grid synchronization for distributed power generation systems." Industrial Electronics, IEEE Transactions on 53.5 (2006): 1398-1409.

[12] Nicastri, A., and A. Nagliero. "Comparison and evaluation of the PLL techniques for the design of the grid-connected inverter systems." Industrial Electronics (ISIE), 2010 IEEE International Symposium on. IEEE, 2010.

[13] Bobrowska-Rafal, M., et al. "Grid synchronization and symmetrical components extraction with PLL algorithm for grid connected power electronic converters-a review." Bulletin of the Polish Academy of Sciences: Technical Sciences 59.4 (2011): 485-497.

[14] Rodriguez, P., L. Sainz, and J. Bergas. "Synchronous double reference frame PLL applied to a unified power quality conditioner." Harmonics and Quality of Power, 2002. 10th International Conference on. Vol. 2. IEEE, 2002.

[15] Rodriguez, P., Pou, J., Bergas, J., Candela, J., Burgos, R. and Boroyevich, D. Decoupled double synchronous reference frame PLL for power converters control. IEEE Transactions on Power Electronics, vol. 22, no. 2, pp. 584-592, 2007.